3D POSITIONING ACCURACY AND LAND COVER CLASSIFICATION PERFORMANCE OF THE UAVS: CASE STUDY OF DJI PHANTOM IV MULTISPECTRAL RTK

Umut Gunes Sefercik[1], Taskin Kavzoglu[1], Ismail Colkesen[1], Samed Adali[1], Salih Dinc[1], Mertcan Nazar[1], Muhammed Yusuf Ozturk[1]
[1]Gebze Technical University, Geomatics Engineering Department, Kocaeli, Turkey,
Email: sefercik@gtu.edu.tr, kavzoglu@gtu.edu.tr, colkesen@gtu.edu.tr

KEY WORDS: UAV, Multispectral, GNSS, RTK, Automatic Land Cover Classification

ABSTRACT: Unmanned air vehicle (UAV) has become an indispensable mobile mapping technology of remote sensing thanks to offering low cost and high resolution spatial data. Particularly, camera equipped optical UAVs are large in demand by land-related professions, including mapping, agriculture and forestry. Regarding the requirements, the technological level of the optical UAVs rises day by day by adding novel payloads. For instance, global navigation satellite system (GNSS) receivers with real-time kinematic (RTK) positioning capability were added to facilitate the fieldwork for ground control point (GCP) set up and measurements before UAV flights. Multispectral cameras were added to increase the automatic land cover classification potential of generated ortho-mosaics. At this point, the most significant question is the contribution level of these technological payloads. In this study, our research group evaluated the RTK GNSS positioning accuracy and automatic land cover classification potential of "DJI Phantom IV Multispectral RTK", which is one of the most common optical UAVs for scientific and commercial applications. For the evaluations, a study area that includes a large variety of land cover classes was selected. The UAV RTK GNSS positioning accuracy was calculated by comparing the RTK GNSS data obtained from the UAV with the measured GCPs in the study area. Furthermore, the land cover classification performance of Multispectral UAV was analysed by pixel and object-based classification techniques separately. For this purpose, while spectral angle mapper (SAM), minimum distance (MD) and maximum likelihood (ML) classifiers were applied to perform pixel-based classification, nearest neighbour (NN) classifier was employed to utilize object-based classification. The positioning accuracy results demonstrated that the root mean square error (RMSE) of UAV RTK GNSS is ±1.1 cm in X, ±2.7 cm in Y, and ±5.7 cm in Z. The classification results showed that the highest overall accuracy was estimated as 93.56% with ML classifier and its classification performance was found to be superior compared to those of SAM (73.46%) and MD (75.27%) classifiers. On the other hand, the overall accuracy was calculated as 90.09% for object-based classification and it was 3% lower than the pixel-based ML classification result. This could be the result of heterogeneity of the image objects created during the segmentation stage. Further studies are required to improve the object-based classification accuracy by applying different segmentation methods and quality measures.

1. INTRODUCTION

Human interference, with its ever-growing magnitude and reach, is one of the biggest factors in the transformation of the Earth's surface and inner structure (Lambin et al., 2001). Land cover is a vital parameter in understanding the impact of human interference on both environment and climate (Foody, 2002; Feddema et al., 2005). Monitoring of land cover change is an important topic in remote sensing with decades of various change detection studies about deforestation, urban growth, land reclamation and general land structure (Tucker et al., 1985; Green et al., 1994; Yuan et al., 2005; Abd El-Kawy et al., 2011; Abdullah et al., 2019). Applying remote sensing approaches like classification methods on satellite or aerial imagery it is possible to obtain information about the land cover classes required for temporal change analysis. Satellite systems generally provide data with limited spatial and temporal resolution. Also, due to high flight costs, traditional airborne methods offer limited temporal resolution (Cömert et al., 2012). Lately, unmanned aerial vehicles (UAVs) which can be controlled remotely without a pilot, are employed as an alternative source apart from satellites and aircraft in land cover classification studies, offering aerial imagery with high spatial and temporal resolution (Sarron et al., 2018; De Luca et al., 2019; Al-Najjar et al., 2019). Providing instantaneous high resolution data with low cost and the capability of producing high quality three dimensional (3D) models and orthomosaic maps increase the interest in UAV technology. UAVs are firstly employed in military operations then thanks to technological advancements, they began to be used in the civilian field. An array of different components can be added to UAVs as the payload such as visual and near-shortwave-mid-thermal infrared cameras, LiDAR (Light Detection and Ranging) scanners, GNSS (Global Navigation Satellite Systems) receivers and other systems for communication. Advanced communication and control systems installed into UAVs provide the ability to carry out autonomous missions using prepared photogrammetric flight plans. Applications such as change analysis, urban planning, disaster management, weather monitoring and agricultural studies can be carried out by deriving information about building areas, road structures, water bodies, residential zones, agricultural fields, and forests from UAV imagery (Altunkaya and Yastıklı, 2011).

Pixels, which are the smallest components of images, display reflection values of objects within a certain area and thus using pixel values, objects can be detected and classified according to their spectral properties. Using multispectral sensors to obtain multiband imagery, reflection properties of objects and surfaces in different spectral bands can be observed. Using multispectral data, which has a significant impact on remote sensing research, various studies and analyses such as crop growth monitoring, soil property examination, water pollution investigation, ship waste monitoring, volcanic studies, and pest detection in forestry (Kavzoğlu and Çölkesen, 2011). As a mainly employed source for multispectral imagery, satellite platforms generally lack in the terms of proving data with high spatial and temporal resolution, especially in studies that require multi-temporal precise data. Ability to obtain multispectral data with high spatial and temporal resolution, UAVs become frequently employed systems in multispectral studies (Doğan and Yıldız, 2019).

In this study, 3D positioning accuracy and pixel-based, object-based land cover classification performance of multispectral UAVs are analysed by using the multispectral data obtained from DJI Phantom IV Multispectral UAV. 3D positioning accuracy was investigated by comparing coordinates of ground control points (GCPs) obtained from terrestrial measurements and UAV real time kinematic (RTK) GNSS data. Land cover classification performance was evaluated by applying pixel-based classification methods such as spectral angle mapper (Girouard et al., 2004), minimum distance (Sisodia et al., 2014), maximum likelihood (Ahmad and Quegan, 2012) and nearest neighbour object-based classification method on 16 independent land cover classes.

2. STUDY AREA AND MATERIALS

The study area is located in Gebze Technical University (GTU) Northern Campus which is in Kocaeli province of Turkey. The area is 500 m × 225 m covering 112.500 m^2 and includes various land cover classes such as farmland, buildings, trees and roads. With the minimum and maximum height above the sea level (orthometric) being 4 m and 20 m, respectively, topography appears mostly flat. Figure 1 shows the location of the study area.

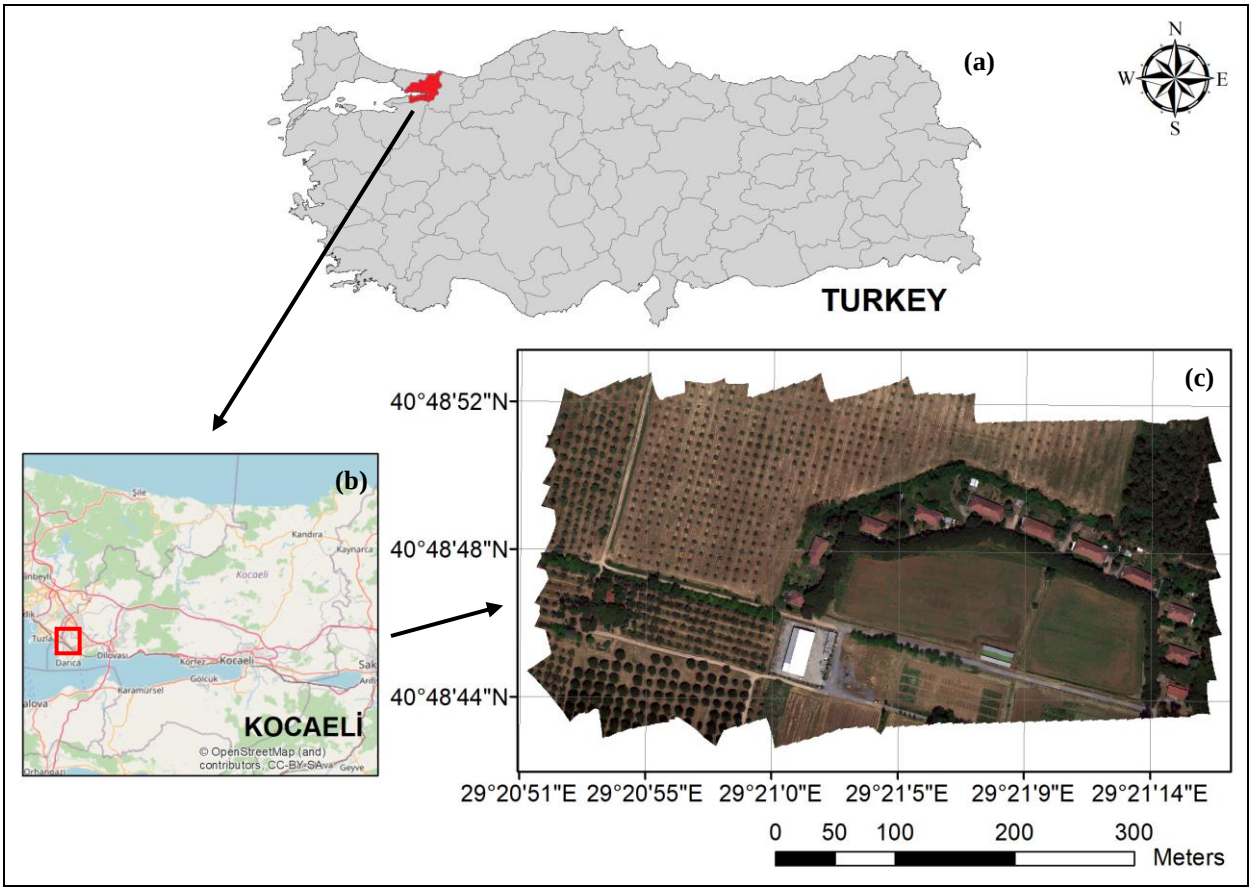

Figure 1. (a) Location of Kocaeli province in Turkey, (b) position of GTU in Kocaeli and (c) orthomosaic map of the study area located in GTU Northern Campus in geographic coordinate system and WGS84 datum

Multispectral aerial photos were acquired by using DJI Phantom IV Multispectral UAV equipped with real time kinematic (RTK) GNSS receiver, accessible at GTU Geomatics Engineering Department's Advanced Remote Sensing Technology Laboratory. The multispectral UAV has six imaging bands consisting of RGB, red, green, blue, red edge and near infrared. Reflectance calibration of multispectral imagery was carried out by utilizing MAPIR Camera Reflectance Calibration Ground Target Package (V2). Figure 2 shows the employed UAV and reflectance calibration targets. Terrestrial measurements were carried out using CHC i80 GNSS receiver which is also available at the laboratory. Specifications of the UAV are given in Table 1.

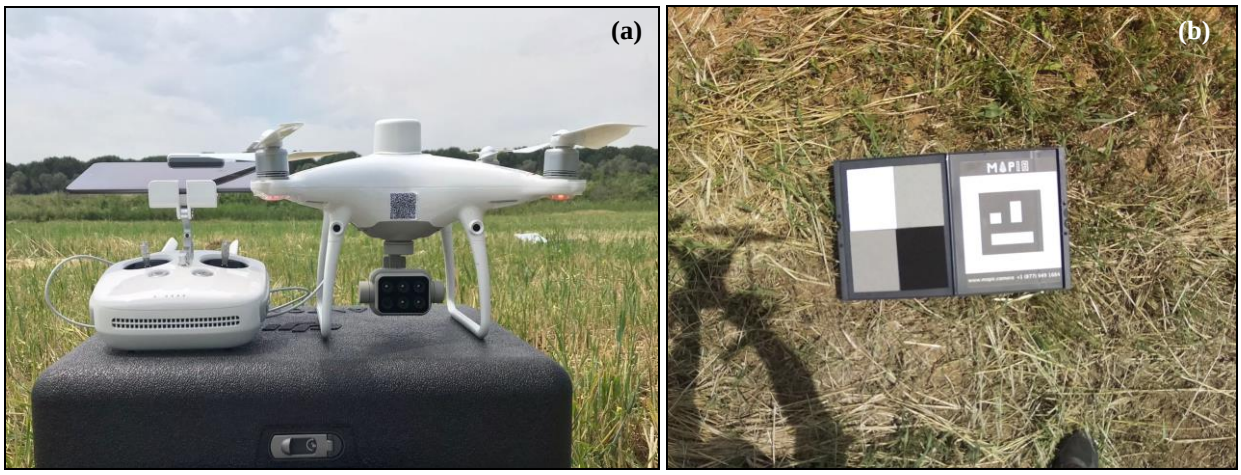

Figure 2. (a) DJI Phantom IV Multispectral UAV and (b) MAPIR Camera Reflectance Calibration Ground Target Package (V2)

Table 1. DJI Phantom IV Multispectral UAV Specifications

	DJI Phantom IV Multispectral UAV
Camera	Six 1/2.9" CMOS sensors including one RGB and five monochrome, effective pixels 2.08 MP
Sensor wavelengths	Blue (B): 450 nm ± 16 nm; Green (G): 560 nm ± 16 nm; Red (R): 650 nm ± 16 nm; Red edge (RE): 730 nm ± 16 nm; Near-infrared (NIR): 840 nm ± 26 nm
Gimbal	3-axis (pitch, roll, yaw)
Flight duration	Max. 27 minutes
Weight	1487 g
Speed	14 m/s (P-mod); 16 m/s (A-mod)
Wind speed resistance	Max. 10 m/s
Operating temperature	0° to 40°C
Outdoor positioning module	GPS, GLONASS, Galileo, Beidou
Hover accuracy range	RTK enabled: ± 0.1 m V, ± 0.1 m H; RTK disabled: ± 0.1 m V, ± 0.3 m H (Vision); ± 0.5 m V, ± 1.5 m H (GPS)
Positioning accuracy RTK	1 cm + 1 ppm Horizontal; 1.5 cm + 1 ppm Vertical

MAPIR Camera Reflectance Calibration Ground Target Package (V2) has 4 targets in different colours, black, dark grey, light grey and white. Table 2 shows the reflectance values of the utilized spectral bands.

Table 2. Reflectance values of the utilized spectral bands for each calibration target

Bands	**Black**	**Dark Gray**	**Light Gray**	**White**
Blue	0.0201364	0.1825563	0.2479796	0.7919165
Green	0.0196304	0.1937623	0.2630370	0.8664320
Red	0.0193714	0.1985430	0.2629007	0.8719577
Red Edge	0.0195625	0.2128809	0.2627409	0.8699902
NIR	0.0214593	0.2283683	0.2754859	0.8625244

3. METHODOLOGY

The methodology of the study consists of three steps as obtaining the UAV data, processing the data and producing orthomosaic and classifying orthomosaic according to land cover classes.

To compare terrestrial measurements with UAV data, 9 GCPs were established over the study area and these GCPs were measured by using Continuously Operating Reference Stations (CORS) Real Time Kinematic (RTK) GNSS method. For aerial photo acquisition, DJI GS (Ground Station) PRO software was used and two polygonal UAV flight plans were prepared. 70 m flight altitude was selected to attain a 3.66 cm ground sampling distance (GSD). The ratios of front and side overlaps were chosen as 80% and 60% respectively. With the flight speed of approximately 4.9 m/s, the capture time interval of aerial photos was set to two seconds. Before the flights were carried out, photos of MAPIR reflectance calibration targets were captured for the reflectance calibration process. Applying the prepared flight plans 530 aerial photos were obtained.

Orientation of aerial photos and dense point cloud generation were done using Agisoft Metashape photogrammetric evaluation software. Agisoft Metashape uses the structure from motion (SfM) technique which is based on the principle of stereoscopic photogrammetry (Dereli et al., 2019; Sefercik et al., 2020). Using a SFM based software, camera position and 3D geometry can be reconstructed by utilizing overlapping photos that were taken from different viewpoints. After the image orientation and dense point cloud generation, the filtering process was carried out to eliminate the noise effect on the dense cloud. After the filtering operation, reflectance calibration of obtained photos was carried out using the reflectance values of utilized spectral bands according to each calibration target. After aerial photos were calibrated, orthomosaic was produced. 3D positioning accuracy was evaluated by comparing GCP coordinates obtained from GNSS surveys and produced orthomosaic which is generated by using RTK GNSS UAV data.

ENVI and eCognition image processing software packages were utilized for the pixel-based and object-based land cover classifications. Supervised classification methods such as maximum likelihood classification (MLC), minimum distance classifier (MDC), and spectral angle mapper (SAM) were utilized for pixel-based classification. As for object-based classification nearest neighbour (NN) method was used. 16 different land cover classes consisting of steppe, grass bush, metal roof, shade, olive, uncultivated land, meadow grass, broadleaf, needle leaf, building tile, building white, rough road, soil, cultivated land, concrete, and water, were determined in the study area. Vegetation indices such as Normalized Difference Vegetation Index (NDVI) and the Normalized Difference Red Edge Index (NDRE) were calculated and applied to 5-band orthomosaic via layer stacking as the 6th and the 7th band, respectively. In the classification process, about the same number of training and test data were collected from the different areas while inspecting the spectral properties of selected pixels. A total of 85693 training and 247152 test data were collected after the process. The total number of training and test data according to each land cover class is given in Table 3.

Table 3. Number of training and test pixels according to each land cover class

Class	Training Pixels	Test Pixels
Steppe	5097	15554
Grass Bush	5506	15674
Metal Roof	5172	15682
Shadow	5879	15838
Olive	5055	15334
Uncultivated Land	5427	15342
Meadow Grass	5031	15811
Broad Leaf	5334	15425
Needle Leaf	5280	15646
Red Roof	5201	15340
White Roof	5123	15389
Gravel Road	5495	15345
Soil	5476	15400
Cultivated Area	5666	15190
Concrete	5115	15163
Water	5836	15019

4. RESULTS

Orthomosaics before and after the reflectance calibration process are shown in Figure 3.

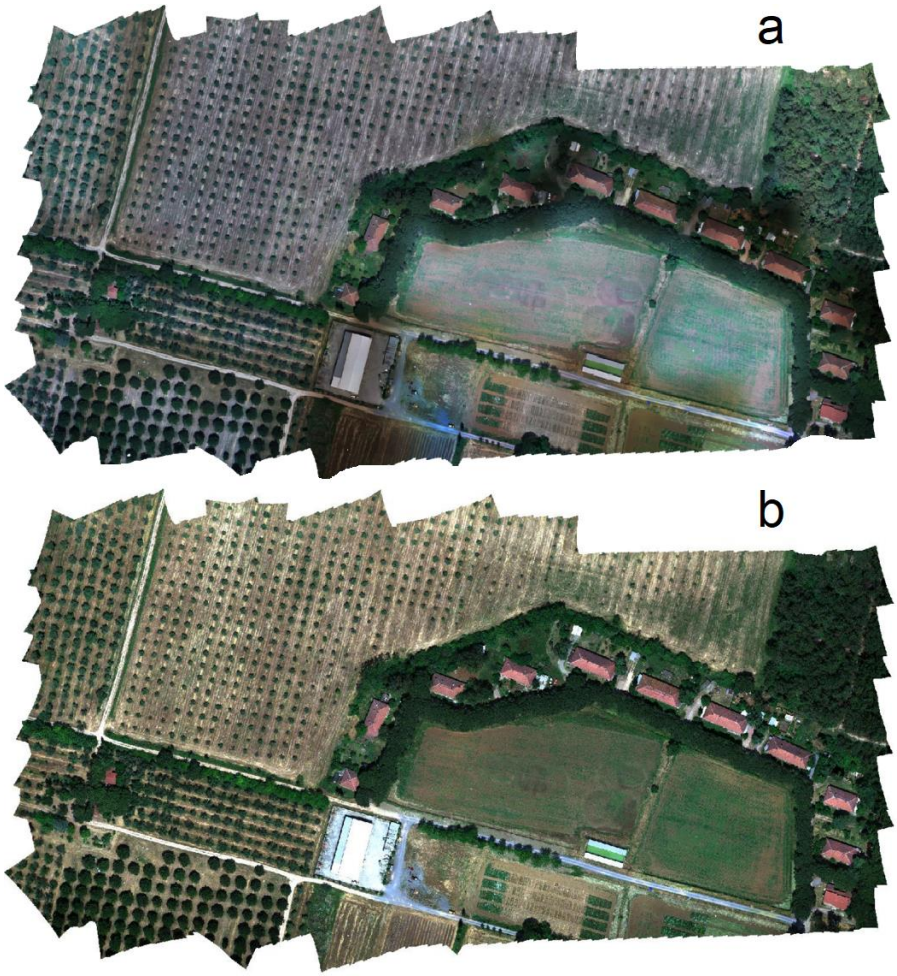

Figure 3. (a) Calibrated orthomosaic and (b) non-calibrated orthomosaic

In Table 4 the results of the comparison of GCP coordinates obtained from terrestrial measurements and selected on generated orthomosaic.

Table 4. Comparison results of GCP coordinates obtained from terrestrial measurements and selected on orthomosaic

GCP	Terrestrial Measurements			UAV RTK GNSS			Errors		
	X (m)	Y (m)	Z (m)	X (m)	Y (m)	Z (m)	ΔX (m)	ΔY (m)	ΔZ (m)
1	445408.933	4520098.918	51.97	445408.944	4520098.875	51.903	-0.011	0.043	0.067
2	445322.326	4519934.34	46.441	445322.331	4519934.339	46.447	-0.005	0.001	-0.006
3	445419.067	4519917.866	45.603	445419.074	4519917.866	45.646	-0.007	0.000	-0.043
4	445044.946	4519962.328	53.575	445044.934	4519962.314	53.550	0.012	0.014	0.025
5	445212.315	4520103.774	52.226	445212.326	4520103.725	52.179	-0.011	0.049	0.047
6	445259.375	4520000.639	48.369	445259.385	4520000.629	48.439	-0.010	0.010	-0.070
7	445406.205	4519969.53	47.736	445406.228	4519969.528	47.800	-0.023	0.002	-0.064
8	445094.118	4520060.561	54.458	445094.124	4520060.516	54.356	-0.006	0.045	0.102
9	445222.708	4519959.093	47.992	445222.710	4519959.089	48.013	-0.002	0.004	-0.021

Comparing the GCP coordinates obtained from the produced orthomosaic with terrestrial measurements root mean square error (RMSE) values were obtained as 1.1 cm in the x-axis, 2.7 cm in the y-axis, and 5.7 cm in the z-axis. With the highest RMSE value in the z-axis, 3D positioning accuracy of the UAV was lower in height direction compared to other directions. The pixel-based SAM, MDC and MLC land cover classification maps are shown in Figure 4.

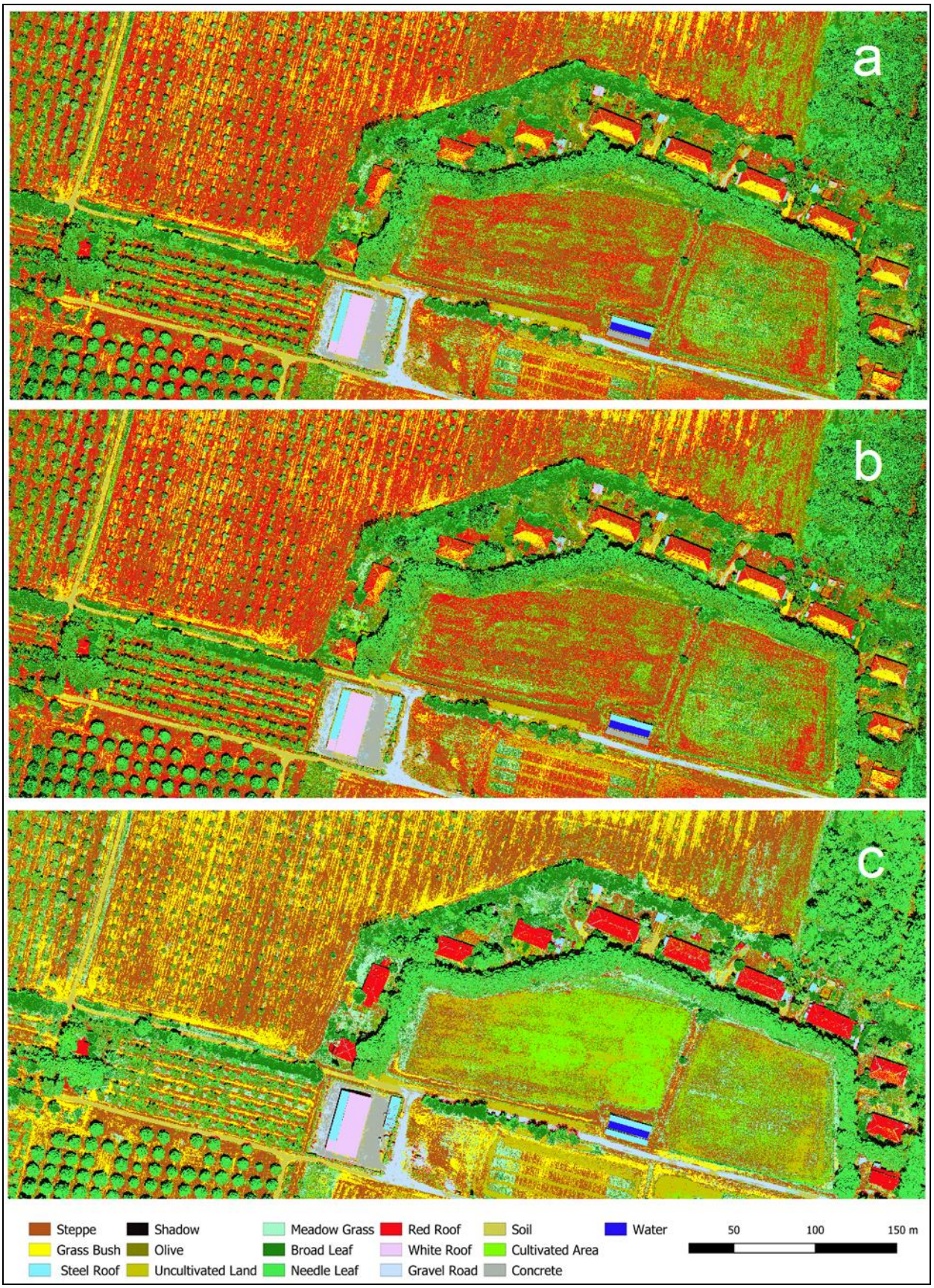

Figure 4. Classification maps of pixel-based methods: (a) SAM, (b) MDC and (c) MLC

The classification accuracies of the pixel-based classification methods SAM, MDC and MLC were 73.46%, 75.27% and 93.56%, respectively. Object-based NN classification map with an accuracy of 90.9% was displayed in Figure 5.

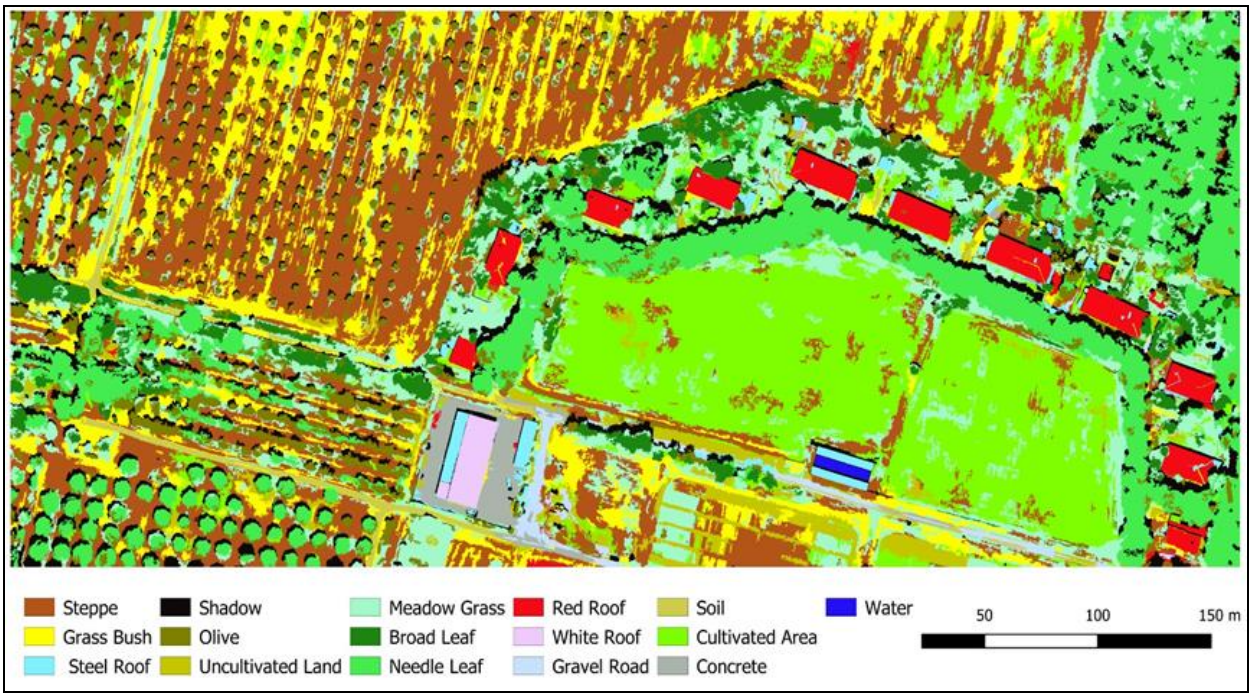

Figure 5. Object based NN classification map

Inspecting the produced classification maps, the land cover classification accuracy of the DJI Phantom IV Multispectral UAV was higher than 90% for both pixel-based and object-based classification methods. In terms of pixel-based classification MLC shows much better performance compared to SAM and MDC, while showing similar results with object-based NN classification method.

5. CONCLUSIONS

Nowadays, UAV technologies are becoming a pinnacle of attraction thanks to their flexibility in using different sensor systems, offering high resolution data with lower cost and less labor compared to other traditional survey methods. Using multispectral UAV systems, the spectral properties of the earth and objects can be obtained with high sensitivity and instantaneously. This study was carried out to evaluate the 3D positioning accuracy and land cover classification performance of multispectral UAVs. To accomplish these tasks, a study area with different land cover classes in GTU Northern Campus was chosen. Before the UAV flights were carried out, 9 GCPs were established over the study area. After GCP measurements were done by GNSS surveys, two UAV flights were carried out using DJI Phantom IV Multispectral UAV and aerial photos were obtained with a GSD of 3.66 cm. Then using reflectance calibration target values for each imaging band used in this study, aerial photos were calibrated and orthomosaic was generated. To evaluate the 3D positioning accuracy of the UAV, GCP coordinates obtained from the terrestrial measurements and produced orthomosaic were compared and RMSE values were calculated as 1.1 cm in the x-axis, 2.7 cm in the y-axis, and 5.7 cm in the z-axis. The pixel-based classification methods SAM, MDC, MLC and object-based classification method NN were applied to produced orthomosaic for inspecting the land cover classification performance. With the highest accuracy of 93.56% the MLC method performed best compared to other pixel-based methods applied, SAM and MDC. The visual interpretation and accuracies of SAM and MDC classification maps were similar, 73.46% and 75.27% respectively. The object-based NN method showed an accuracy of 90.9%, demonstrating a similar result to MLC. Overall, the orthomosaic produced by using aerial imagery obtained from DJI Phantom IV Multispectral UAV displayed higher accuracy than 90% for both pixel-based and object-based land cover classification.

ACKNOWLEDGEMENTS

We would like to thank TÜBİTAK for supporting this study within the scope of the 2209-A University Students Research Projects Support Program.

REFERENCES

Abd El-Kawy, O. R., Rød, J. K., Ismail, H. A., Suliman, A. S., 2011. Land use and land cover change detection in the western Nile delta of Egypt using remote sensing data. Applied Geography, 31(2), pp. 483-494.

Abdullah, A. Y. M., Masrur, A., Adnan, M. S. G., Baky, M., Al, A., Hassan, Q. K., Dewan, A., 2019. Spatio-temporal patterns of land use/land cover change in the heterogeneous coastal region of Bangladesh between 1990 and 2017. Remote Sensing, 11(7), pp. 790.

Ahmad, A., Quegan, S., 2012. Analysis of maximum likelihood classification on multispectral data. Applied Mathematical Sciences, 6(129), pp. 6425-6436.

Al-Najjar, H. A., Kalantar, B., Pradhan, B., Saeidi, V., Halin, A. A., Ueda, N., Mansor, S., 2019. Land cover classification from fused DSM and UAV images using convolutional neural networks. Remote Sensing, 11(12), pp. 1461.

Altunkaya, Z., Yastıklı, N., 2011. Ortogörüntüler yardımıyla nesne tabanlı sınıflandırma yöntemi kullanılarak öznitelik çıkarımı. In TMMOB Geographic Information Systems Congress, Antalya, Turkey.

Cömert, R., Avdan, U., Şenkal, E., 2012. İnsansız hava araçlarının kullanım alanları ve gelecekteki beklentiler. In 4th Remote Sensing and Geographic Information Systems Symposium, Zonguldak, Turkey.

De Luca, G., N Silva, J. M., Cerasoli, S., Araújo, J., Campos, J., Di Fazio, S., Modica, G., 2019. Object-based land cover classification of cork oak woodlands using UAV imagery and Orfeo ToolBox. Remote Sensing, 11(10), pp. 1238.

Dereli, M. A., Polat, N., Uysal, M., 2019. Düşük maliyetli İHA ile yüksek çözünürlüklü SYM üretimi. Nevşehir Bilim ve Teknoloji Dergisi, 8(1), pp. 56-62.

Doğan, Y., Yıldız, F., 2019. İHA ile multispektral kameralardan sağlanan görüntüler yardımıyla bitki türlerinin sınıflandırılması. Türkiye İnsansız Hava Araçları Dergisi, 1(1), pp. 15-22.

Feddema, J. J., Oleson, K. W., Bonan, G. B., Mearns, L. O., Buja, L. E., Meehl, G. A., & Washington, W. M., 2005. The importance of land-cover change in simulating future climates. Science, 310(5754), pp. 1674-1678.

Foody, G. M., 2002. Status of land cover classification accuracy assessment. Remote Sensing of Environment, 80(1), pp. 185-201.

Girouard, G., Abdou, B., El Harti, A., Desrochers, A. 2004. Validated spectral angle mapper algorithm for geological mapping: comparative study between QuickBird and Landsat-TM. In XXth ISPRS congress, geo-imagery bridging continents, Istanbul, Turkey.

Green, K., Kempka, D., Lackey, L., 1994. Using remote sensing to detect and monitor land-cover and land-use change. Photogrammetric Engineering and Remote Sensing, 60(3), pp. 331-337.

Kavzoğlu, T., Çölkesen, İ., 2011. Uzaktan algılama teknolojileri ve uygulama alanları. In Sustainable Land Management Workshop in Turkey, Istanbul, Turkey.

Lambin, E. F., Turner, B. L., Geist, H. J., Agbola, S. B., Angelsen, A., Bruce, J. W., ..., Xu, J., 2001. The causes of land-use and land-cover change: moving beyond the myths. Global Environmental Change, 11(4), pp. 261-269.

Sarron, J., Malézieux, É., Sané, C. A. B., Faye, É., 2018. Mango yield mapping at the orchard scale based on tree structure and land cover assessed by UAV. Remote Sensing, 10(12), pp. 1900.

Sefercik, U. G., Tanrikulu, F., Atalay, C., 2020. SFM Tabanlı Yeni Nesil Görüntü Eşleştirme Yazılımlarının Fotogrametrik 3B Modelleme Potansiyellerinin Karşılaştırması. Türkiye Fotogrametri Dergisi, 2(2), pp. 39-45.

Sisodia, P. S., Tiwari, V., Kumar, A., 2014. A comparative analysis of remote sensing image classification techniques, International Conference on Advances in Computing, Communications and Informatics (ICACCI), pp. 1418-1421.
Tucker, C. J., Townshend, J. R., Goff, T. E., 1985. African land-cover classification using satellite data. Science, 227(4685), pp. 369-375.

Yuan, F., Sawaya, K. E., Loeffelholz, B. C., Bauer, M. E., 2005. Land cover classification and change analysis of the Twin Cities (Minnesota) Metropolitan Area by multitemporal Landsat remote sensing. Remote Sensing of Environment, 98(2-3), pp. 317-328.